Terminal Phase Guidance Design for an Anti-Ship Bank-To-Turn (BTT) Cruise Missile

N. Akilandeswari[1*], Mallikarjun. Bangi[1*], K.K. Mangrulkar[2], and G. Naresh Kumar[3]

[1]Engineer, Hyderabad, Telangana, India,
[1]Associate Professor, DIAT, Pune, Maharashtra, India,
[3]Scientist, DRDL, Hyderabad, Telangana, India,

Abstract

In this paper, a different approach guidance technique is evolved by generating an angle, to guide an anti-ship cruise missile in terminal phase. The present work focuses to model and simulate a guidance scheme for terminal phase of an anti-ship Bank to Turn (BTT) cruise missile. The targeted ships are relatively slow compared to missile speeds. The modified guidance law of Pure Pursuit and Proportional Navigation (PN) in terms of course angle is implemented for stationary as well as moving targets in the lateral plane. The longitudinal guidance is achieved by computing the commanded altitude as a function of range to go.

Keywords: *Course Angle, Bank-to-Turn, Proportional Navigation, Pure Pursuit*

1. Introduction

Anti-ship missiles are guided missiles designed to attack moving ship targets. The target ships are relatively slow moving with respect to the interceptor. Hence, cruise missiles are designed to maintain constant speed over a long range where maneuverability is not a primary concern. They are categorized into Bank-To-Turn (BTT) missiles as they have wings and mimic an aircraft. In order to change the direction of flight, the vehicle banks, generating a component of lift along the lateral axis. Guidance forms a major component of the missile system. The reasons for perturbation in trajectory arise due to motion of target, launching errors, external and internal disturbances.

Guidance of BTT missiles is a widely researched topic. Proportional navigation (PN) is commonly used guidance law for anti-ship missiles. Biased Proportional Navigation (BPN) is proved superior to PN in presence of sensor noise. Jang et.al Jang Gyu Lee, Hyung Seok Han, and Young Jin Kim (1999) attempted to analyse and make a comparison of PN and BPN laws. Kent B. Watterson Kent B. Watterson (1983), discussed mainly about baseline guidance scheme with a pop-up maneuver, and sea-skimming guidance scheme. In his work, for terminal homing. PN guidance is used in azimuth plane and altitude hold cruising in elevation plane. It is also stated that PN is used separately in yaw and pitch plane at terminal impact phase. Cunningham, EP (1974) devised a zero heading error scheme and stated that, it is better than 3-D PN guidance by generating roll and pitch acceleration commands. A guidance law using Lyapnov function is formulated by Tae et.al Tae Soo No, John E. Cochran, Jr. and Eul Glon Kim (2001) where he explained about computing roll angle and pitch acceleration using non-zero effort miss by eliminating polar conversion and he also compared it with PN.

Terminal phase of BTT missile guidance along with impact angle and impact time constraints have been emphasized in works Qingchun Li, Wensheng Zhang, Gang Han and Yehui Yang (2015), Wei Lei, Shunli Li, and Yuqi Zhao (2012) and Hyo-Sang Shin, Jin Ik Lee, and Min-Jea Tahk (2006).

*Corresponding Author: Email: mallikarjun.bangimatam@gmail.com

Many guidance laws are evolved either to improve the guidance performance of the conventional Proportional Navigation and Pure Pursuit Guidance law are to achieve some specific requirements. Normally, BTT missile guidance involves conversion from Cartesian coordinates to roll angle and pitch acceleration using Polar Conversion Logic (PCL).

2. Problem Definition

The objective of all navigation, guidance and control (NGC) systems had been that the control system is designed efficiently to make the air frame follow the generated commands. The guidance system provides the necessary corrections in the flight path which are then translated to mechanical commands to the system's actuators by the autopilot. The vehicle considered is a BTT subsonic cruise missile with 0.75 Mach, which can be launched from multiple platforms. Its launch phase involves a solid propellant and once it enters cruise phase, the wings are deployed and the propulsion is switched to a turbofan engine.

The BTT missile guidance commonly involves conversion from Skid-To-Turn (STT) commands to pitch acceleration and roll angle. A course angle autopilot is suggested in place of a lateral acceleration autopilot in horizontal/yaw plane. The guidance is achieved using line of sight angle in yaw plane. Guidance algorithm generates course angle, which is provided as input to the autopilot. Here, an attempt is made to implement the same using different guidance laws, mainly Pure pursuit guidance, deviated pursuit guidance and with Proportional Navigation guidance.

3. Mathematical Modelling

A non-linear 6-DOF model of the missile using Newton-Euler method is used for simulation. Typical axis convention for BTT missile using right handed co-ordinate system is shown in fig. 1. The body axis frame is denoted by (XB, YB, ZB) while the inertial co-ordinate frame is represented in NED Frame.

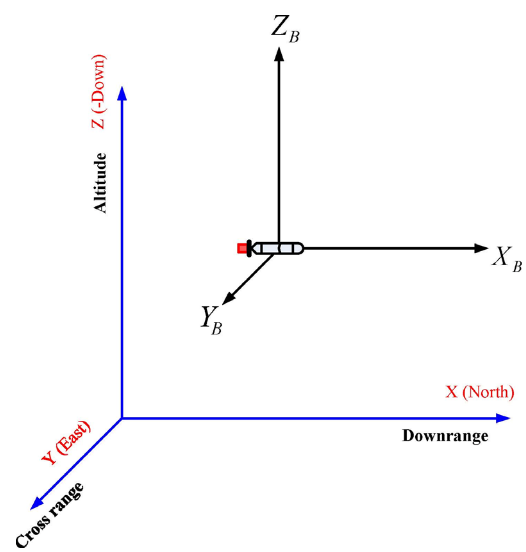

Figure 1: Axis convention of a missile

The various assumptions considered for analysis include:

1) The earth is at, non-rotating and is fixed in inertial space.
2) The atmospheric density is constant.
3) The vehicle is a rigid body.
4) The mass is constant as the fuel consumed by the turbofan engine is less and their effects are neglected.
5) The rate of change of inertia is negligible.
6) The thrust is assumed to be aligned with the center line of body X-axis and hence creates no moment about the center of mass of the vehicle.
7) As the missile is symmetric along both XY-plane and XZ-plane, the product of moments of Inertia IXY and IY Z are considered to be zero.

3.1 MISSILE EQUATIONS OF MOTION

The mathematic model Randal W Beard and Timothy W McLain (2012) of a generic BTT missile is derived in this section. The non-linear translational kinematic equations that relate the inertial velocities $(\dot{p}_n, \dot{p}_e, \dot{p}_d)$ with the body frame velocities (u, v, w) are represented as:

$$\begin{aligned}
\dot{p}_n &= u\cos\theta\cos\phi + v(\sin\phi\sin\theta\cos\psi - \cos\phi\sin\psi) + w(\cos\phi\sin\theta\cos\psi + \sin\phi\sin\psi) \\
\dot{p}_e &= u\cos\theta\sin\psi + v(\sin\phi\sin\theta\sin\psi + \cos\phi\cos\psi) + w(\cos\phi\sin\theta\sin\psi - \sin\phi\cos\psi) \\
\dot{p}_d &= -u\sin\theta + v(\sin\phi\cos\theta) + w(\cos\phi\cos\theta)
\end{aligned} \tag{1}$$

The non-linear relationship between the Euler angle rates $(\dot{\phi}, \dot{\theta}, \dot{\psi})$ and angular velocities (p, q, r) is given by the following kinematic equations:

$$\begin{aligned}
\dot{\phi} &= p + q\sin\phi\tan\theta + r\cos\phi\tan\theta \\
\dot{\theta} &= q\cos\phi - r\sin\phi \\
\dot{\psi} &= q\sin\phi\sec\theta + r\cos\phi\sec\theta
\end{aligned} \tag{2}$$

The six-DOF equations of motion of the flight vehicle are

$$\begin{aligned}
\dot{u} &= rv - qw + \frac{F_x}{m} \\
\dot{v} &= pw - rq + \frac{F_y}{m} \\
\dot{w} &= qu - pv + \frac{F_z}{m} \\
\dot{p} &= \frac{I_{xz}(I_x - I_y + I_z)}{I_x I_z - I_{xz}^2} pq - \frac{I_z(I_z - I_y) + I_{xz}^2}{I_x I_z - I_{xz}^2} qr + \frac{I_z}{I_x I_z - I_{xz}^2} M_x + \frac{I_z}{I_x I_z - I_{xz}^2} M_x \\
\dot{q} &= \frac{(I_z - I_x)}{I_y} pr - \frac{I_{xz}}{I_y}(p^2 - r^2) + \frac{M_x}{I_y} \\
\dot{r} &= \frac{I_z(I_z - I_y) + I_{xz}^2}{I_x I_z - I_{xz}^2} pq - \frac{I_{xz}(I_x - I_y + I_z)}{I_x I_z - I_{xz}^2} qr + \frac{I_{xz}}{I_x I_z - I_{xz}^2} M_x + \frac{I_x}{I_x I_z - I_{xz}^2} M_x
\end{aligned} \tag{3}$$

Here, M_x, M_y and M_z represents the rolling, pitching and yawing moments about body X, Y and Z axes respectively while F_x, F_y and F_z represent the forces along body X, Y, and Z axes respectively. The dynamics of the flight vehicle are described by the following force and moment equations along the three co-ordinate axes.

$$M_x = QbSC_1, M_y = QbSC_m, M_z = QbSC_n \tag{4}$$

Where the moment co-efficient are given by the following equation:

$$\begin{pmatrix} C_1 \\ C_m \\ C_n \end{pmatrix} = \begin{pmatrix} C_{10} \\ C_{m0} \\ C_{n0} \end{pmatrix} + \begin{pmatrix} 0 & C_{l\beta} \\ C_{m\alpha} & 0 \\ 0 & C_{n\beta} \end{pmatrix} \begin{pmatrix} \alpha \\ \beta \end{pmatrix} + \frac{1}{2V_m} \begin{pmatrix} bC_{lp} & 0 & bC_{lr} \\ 0 & cC_{mq} & 0 \\ bC_{n_p} & 0 & bC_{n_r} \end{pmatrix} \begin{pmatrix} p \\ q \\ r \end{pmatrix} + \begin{pmatrix} C_{l\delta a} & 0 & C_{l\delta r} \\ 0 & C_{m\delta e} & 0 \\ C_{n\delta a} & 0 & C_{n\delta r} \end{pmatrix} \begin{pmatrix} \delta_a \\ \delta_e \\ \delta_r \end{pmatrix} \tag{5}$$

Here, $C_{l\beta}, C_{m\alpha}, and\ C_{n\beta}$ are known as the stability derivatives due to the effect of angle of attack (α) and side slip angle (β) while C_{lp}, C_{mq} and C_{nr} act as the damping derivatives. Also, $C_{l\delta a}, C_{m\delta e}, and\ C_{n\delta r}$ associated with the control surface deflections are called the primary control derivatives while $C_{l\delta a}, and\ C_{n\delta a}$ are known as the cross control derivatives that effect due to the coupling of roll and yaw motions. Similarly, the forces along various axes are given by:

$$\begin{pmatrix} F_x \\ F_y \\ F_z \end{pmatrix} = QS \begin{pmatrix} \sin\alpha & 0 & -\cos\alpha \\ 0 & 1 & 0 \\ -\cos\alpha & 0 & -\sin\alpha \end{pmatrix} \begin{pmatrix} C_L \\ C_Y \\ C_D \end{pmatrix} + \begin{pmatrix} T \\ 0 \\ 0 \end{pmatrix} + \begin{pmatrix} G_x \\ G_y \\ G_Z \end{pmatrix} \qquad (6)$$

The dynamic pressure at a velocity 'Vm' is given by: $Q = \frac{1}{2}\rho V_m{}^2 \qquad (7)$

Here, the aerodynamic force co-efficients are described by

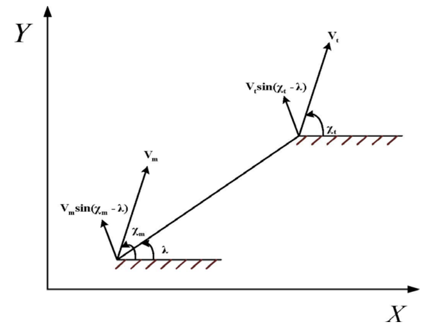

Figure 2: PN Guidance law in lateral plane

$$\begin{pmatrix} C_L \\ C_Y \\ C_D \end{pmatrix} = \begin{pmatrix} C_{L0} \\ C_{Y0} \\ C_{D0} \end{pmatrix} + \begin{pmatrix} C_{L\alpha} & 0 \\ 0 & C_{Y\beta} \\ C_{D\alpha} & 0 \end{pmatrix} \begin{pmatrix} \alpha \\ \beta \end{pmatrix} + \frac{1}{2V_m} \begin{pmatrix} 0 & cC_{Lq} & 0 \\ 0 & cC_{Dq} & 0 \\ bC_{Yp} & 0 & bC_{Yr} \end{pmatrix} \begin{pmatrix} p \\ q \\ r \end{pmatrix} + \begin{pmatrix} 0 & C_{L\delta e} & 0 \\ C_{Y\delta\alpha} & 0 & C_{Y\delta r} \\ 0 & C_{D\delta e} & 0 \end{pmatrix} \begin{pmatrix} \delta_\alpha \\ \delta_e \\ \delta_r \end{pmatrix} \qquad (8)$$

Here, $C_{L\alpha}, C_{D\alpha}, C_{Y\beta}, C_{Lq}, C_{Dq}, C_{Yp}, and\ C_{Y\alpha}$ are known as the stability derivatives. $C_{L\delta_e}, C_{D\delta_e}, C_{Y\delta_a}, C_{Y\delta_r}$ are called as control derivatives. Thrust is assumed to be oriented along the nose of the missile. The gravity components in Eqn. 6 along the axes in body frame is represented as

$$\begin{pmatrix} G_x \\ G_y \\ G_z \end{pmatrix} = mg \begin{pmatrix} -\sin\theta \\ \cos\theta\sin\phi \\ \cos\theta\cos\phi \end{pmatrix} \qquad (9)$$

3.2 MISSILE PARAMETERS

The following data is used for simulation: Kent B. Watter-son (1983). The elevator, aileron and rudder deflections are limited to ±15.

Table 1: Missile Parameters

S.No.	Parameter	Data	Units	S.No.	Parameter	Data	Units
1	Wing span, 'b'	2.58622	m	7	I_x	37.691731	kgm^2
2	Platform area, 'S'	1.11484	m^2	8	I_y	2043.217	kgm^2
3	Maximum chord 'c'	0.43098	m	9	I_z	2043.996	kgm^2
4	Missile velocity, "V_m"	255.72	ms^{-1}	10	I_{xz}	15.8630	kgm^2
5	Sea level Density, "p"	1.22505	kgm^{-3}	11	Thrust	2668.993	N
6	Mass of the missile, "m"	1000	kg				

3.3 Seeker Model

Consider the 2D engagement geometry in a yaw plane as shown in fig 2. The components of relative missile to target separations along X and Y co-ordinates are expressed below:

$$\Delta X = X_t - X_m,\ \Delta Y = Y_t - Y_m \qquad (10)$$

Where (X_m & Y_m) are the missile positions, and (X_t & Y_t) are the target positions along north and east respectively. The relative velocity components in Earth co-ordinates are given by

$$\Delta V_x = V_{tx} - V_{mx},\ \Delta V_y = V_{ty} - V_{my} \qquad (11)$$

Where (V_{mx} & V_{my}) are the missile velocities and (V_{tx} &V_{ty}) are the target velocities along north and east respectively.

The relative separation or the relative range-to-go `R' between missile and target expressed in terms of its inertial components as

$$R = \sqrt{\Delta X^2 + \Delta Y^2} \qquad (12)$$

Differentiating the above equation, the closing velocity `Vc' is expressed as:

$$V_c = \frac{-\Delta X \times \Delta V_x + \Delta Y + \Delta V_y}{R} \qquad (13)$$

The Line of Sight (LOS) angle, `λ' and line of sight rate, `$\dot{\lambda}$' are expressed in terms of relative separation components as:

$$\lambda = \tan^{-1}\left(\frac{\Delta Y}{\Delta X}\right) \qquad (14)$$

$$\dot{\lambda} = \frac{\Delta X \times \Delta V_y - \Delta Y \times \Delta V_x}{R^2} \qquad (15)$$

3.4 Representation of Course Angle

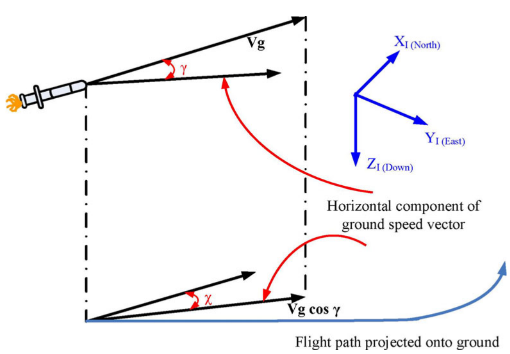

Figure 3: Visualization of Course angle

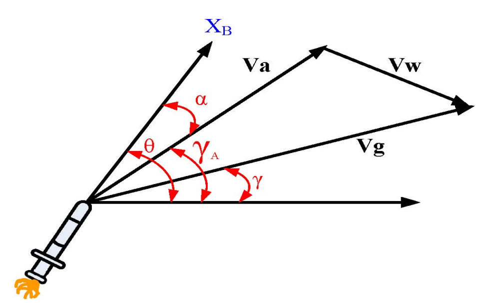

Figure 4: Schematic in Vertical plane

The direction of the ground speed vector relative to inertial frame as seen in fig. 3 is specified using two angles viz. the course angle (X) and the flight path angle (γ). Fig. 4 shows the flight path angle between the horizontal plane and the ground velocity vector V_g, while the course is the angle between the projection of the ground velocity vector onto the horizontal plane and true north as shown in fig. 5. The simulation is carried out in MATLAB

ISBN - 978-93-95038-50-8

using Runge-Kutta-4 (RK4) method. When the altitude falls below ground level and when the instantaneous relative range between targets to missile is higher than its previous recorded value indicating that the missile is receding away from the target act as stopping criteria of simulation.

The maximum target velocity is assumed to be 30 m/s.

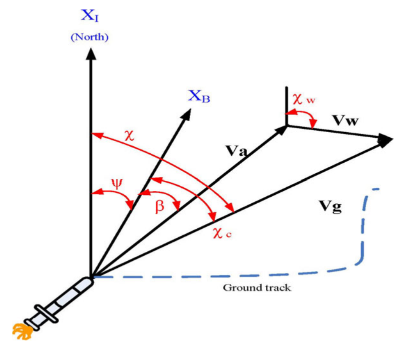

Figure 5: Schematic in Horizontal plane

4. Guidance Techniques

The target ship's manoeuvrability and speed are negligible with those of anti-ship missiles which attain high-subsonic or supersonic speeds. Assumed that the missile speed is constant throughout the engagement. Guidance design assumes seeker to provide (λ), ($\dot{\lambda}$), (R) and (V_c) between the missile and target as inputs to the system. It is implemented separately in 2D planes i.e., in lateral (yaw-plane) and longitudinal (pitch-plane) guidance separately. Pure pursuit, Deviated pursuit and Proportional navigation guidance are used in the lateral plane. For altitude guidance, an altitude profile depending on relative range is generated and used as the commanded reference. The outputs are directed to second-order autopilot [7].

4.1 Pure Pursuit Guidance

Table 2: Pure Pursuit Guidance

Initial X_t (km)	Initial Y_t (km)	V_{tx} (m/s)	V_{ty} (m/s)	Miss Distance (m)
5	0.1	0	0	0.09899
5	0.5	0	0	0.08864
5	0.1	0	10	13.41
8	0.5	0	0	0.02358
8	0.2	0	0	0.08077
5	0.1	0	30	90.94

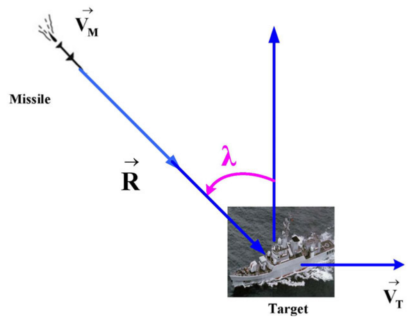

Figure 6: Pure pursuit guidance law

In principle, the pure pursuit guidance states that if the pursuer keeps pointing at the target, it shall collide with the target at one point, if the missile's velocity vector points at the target's current position at every instant of time. It is implemented by commanding the required course angle of the missile to be the line of sight angle between the missile and target as shown in fig 6 obtained from the seeker. $X = \lambda$ (16)

Table 3. Deviated Pursuit Guidance with k_λ=8

Initial X_t (km)	Initial Y_t (km)	V_{tx} (m/s)	V_{ty} (m/s)	Miss Distance
5	0.5	5	10	0.8045 m
5	0.1	0	10	0.8401 m
5	0.1	0	30	3.153 m
5	0.1	0	0	0.7033 m

While pure pursuit guidance works well with stationary targets, an anticipation is required to track the target in case of moving targets.

Results: Few test cases are simulated using pure pursuit guidance and the result is tabulated below in Table 2. The results show that as the target is simulated with a velocity, miss distances are huge for moving targets.

4.2 Modified Deviated Pursuit Guidance

Table 4. Deviated Pursuit Guidance with Filter of DC Gain=1 and Time constant T=10

Initial X_t (km)	Initial Y_t (km)	V_{tx} (m/s)	V_{ty} (m/s)	Miss Distance (m)
5	0.5	5	10	0.8118
5	0.1	0	10	1.079
5	0.1	0	30	19.15
5	0.1	0	0	0.01144

Deviated pursuit is a form of pursuit guidance, there is a constant additional deflection added to the pure pursuit input. An (k_λ) additional term is introduced which is continuously varying along the missile downrange. The LOS rate is multiplied by a gain

ISBN - 978-93-95038-50-8

factor and is added to the LOS angle (pure pursuit input), thus calculating the required commanded course angle. $X = \lambda + k_{\lambda}\dot{\lambda}$ (17)

But, the miss distances depend upon the target velocity and relative initial error along the y-direction between missile and target in the inertial frame. The control demand from guidance loop increases as the missile approaches the target. A low pass filter of the form $\left[\frac{a}{s+a}\right]$ is added to the product of gain and LOS rate, with different filter time constants to remove high frequencies. The errors do not have a pattern and result in huge miss distances for some cases. Limiting the filter output or introducing non-linear gain at different ranges were not useful.

Results Few test cases are studied and the results have been tabulated in Table 3. A filter was added to the product of gain and rate of line of sight but errors changed depending on different filter time constants, and did not show a pattern. Large miss distances were found from case to case. Limiting the filter output or introducing non-linear gain at different ranges were not improving miss distances. Some of the cases are tabulated in Table 4.

4.3 Proportional Navigation Guidance

By definition of Proportional Navigation (PN), the rate of change of line of sight (LOS) angle is zero. PN Guidance using Course Angle in order to achieve zero rate of change of LOS, the missile's velocity component perpendicular to the line of sight must be equal to the target's velocity component perpendicular to the line of sight.

$$V_m \sin(X_m - \lambda) = V_t \sin(X_t - \lambda) \quad (18)$$

$$Resolving\,(X_t - \lambda)\; X_m = \lambda + \sin^{-1}\left(\frac{V_{ty}\cos\lambda - V_{tx}\,sin\lambda}{V_m}\right) \quad (19)$$

Proportional Navigation Guidance Using Roll Angle

By directly using roll angle, fig. 7 shows the block diagram of PN guidance law implementation.

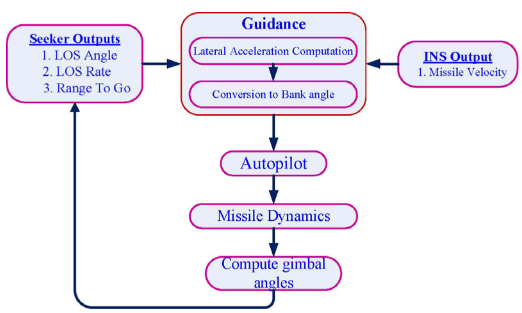

Figure 7: Block diagram of PN Guidance

$$a_c = N'V_c\dot{\lambda} \quad (22)$$

Re-writing lateral acceleration in terms of course angle is

$$V_m\dot{X} = N'V_c\dot{\lambda} \quad (23)$$

Assuming V_m ? V_t, and hence. $V_c = V_m \Rightarrow \dot{X} = N'\dot{\lambda}$ (24)

ISBN - 978-93-95038-50-8

Relating $\dot{\chi}$ and $\phi \Rightarrow \phi = \tan^{-1}\left(\frac{N' V_m \dot{\chi}}{g}\right) = \tan^{-1}\left(\frac{\dot{\chi} V_m}{g}\right)$ (25) This is limited to a maximum of ±30° and given as input to the roll autopilot directly.

Results: Few test cases have been simulated and results are tabulated in Table 5.

Table 5. PN Guidance using Course Angle

Initial X_t (km)	Initial Y_t (km)	V_{tx} (m/s)	V_{ty} (m/s)	Miss Distance
5	0.5	5	10	0.1232 m
5	0.2	0	30	0.1041 m
5	0.5	30	30	0.0250 m
5	0.1	0	30	0.0459 m
5	0.1	0	0	0.0989 m
5	0.1	0	10	0.0126 m

Designed a math model by representing lateral acceleration in terms of course angle, and directly commanding roll autopilot were developed. A test case was generated by following assumptions with initial distances 5 km and 0.5 km along inertial X-axis and Y-axis respectively with target velocity along north is 10 m/s and along east it is to be 30 m/s, and with Navigation Constant (N) = 3, the simulation were carried out and observed a miss distance error as 0.07913 metres.

4.4 COLLISION TRIANGLE IN PN GUIDANCE

For a simulation case using PN guidance, with initial target co-ordinates (Xt &Yt) of (5km&0.1km) and with initial velocity of 10m/s along the east direction, the miss distance and altitude error turns out to be 0.1237 m and 0.1840 m respectively.

The engagement trajectory is shown below in fig. 8. When the rate of change of line of sight becomes zero, the missile gets onto the collision course, and from then the current LOS remains parallel to the previous LOS. Data of missile and target positions have been generated for every 0.5 sec and the collision triangle is plotted in fig. 9.

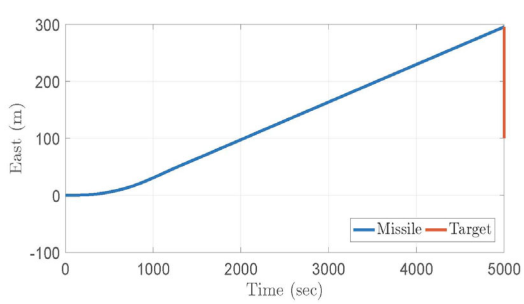

Figure 8: Trajectory

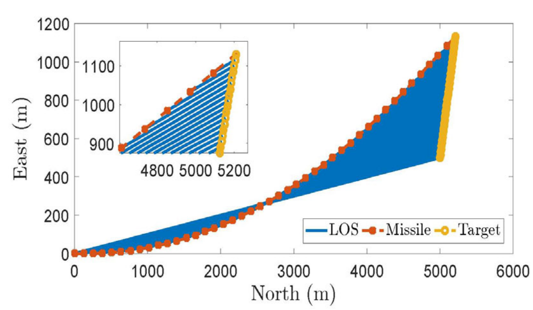

Figure 9: Collision Triangle

4.5 LONGITUDINAL GUIDANCE

In the longitudinal plane, a reference altitude signal needs to be generated from the start of terminal phase. Let h_0 and R_0 be the altitude and horizontal range at the start of terminal phase. The commanded altitude h_c needs to be proportional to the instantaneous horizontal

ISBN - 978-93-95038-50-8

range. Assuming the target height is around 3 m, we aim to hit at 1.5 m and hence, we have,

$$\frac{h_c - 1.5}{h_o - 1.5} = \frac{R}{R_o} \Rightarrow h_c = \frac{h_o - 1.5}{R_o} R + 1.5 \quad (26)$$

On generalizing at every instant of time, $h_c = \frac{h_o - 1.5}{R_o}\left(R + \dot{R}dt\right) + 1.5 \quad (27)$

Thus, a smooth ramp signal is generated as the commanded reference such that the missile dives close to sea level only near to the point of engagement.

5. CONCLUSION

The guidance design using course angle is implemented in lateral and longitudinal planes separately. Guidance in the horizontal plane is achieved by modification of two different guidance principles. Analyses with various test cases show that final errors in miss distance at the point of impact are comparable thus indicating the robustness of the algorithm. Further, the work may be expanded into many areas including incorporating seeker model, including seeker noise and sea-clutter in the background.

ACKNOWLEDGEMENT

The authors thank competent authorities of Defence Research and Development Laboratory (DRDL), Hyderabad for granting permission to publish this piece of work.

REFERENCES

1. Cunningham, EP (1974). Guidance of a bank-to-turn missile with altitude control requirements. Journal of Spacecraft and Rockets, 11(5), 340-342.
2. Hyo-Sang Shin, Jin Ik Lee, and Min-Jea Tahk (2006). Guidance synthesis to control impact angle and time. KSAS International Journal, 7(1), 129-136.
3. Jang Gyu Lee, Hyung Seok Han, and Young Jin Kim (1999). Guidance performance analysis of bank-to-turn (btt) missiles. International Conference on Control Applications, 991-996.
4. Kent B. Watterson (1983). Bank-to-turn cruise missile terminal guidance and control law comparison. Ph.D. thesis, Naval Postgraduate School Monterey, California.
5. Paul Zarchan (2012). Tactical and strategic missile guidance, volume 157. American Institute of Aeronautics and Astronautics, Inc.
6. Qingchun Li, Wensheng Zhang, Gang Han and Yehui Yang (2015). Adaptive neuro-fuzzy sliding mode control guidance law with impact angle constraint. IET Control Theory and Applications, 09(14), 2115{2123. doi:10.1049/iet-cta.2014.1206.
7. Randal W Beard and Timothy W McLain (2012). Navigation, Guidance, and Control of Small Unmanned Air-craft. Princeton university press.
8. Tae Soo No, John E. Cochran, Jr. and Eul Glon Kim (2001). Bank-to-turn guidance law using Lyapnov function and nonzero effort miss. Journal of Guidance, Control, and Dynamics, 24(02), 255-260.
9. Wei Lei, Shunli Li, and Yuqi Zhao (2012). Design of anti-ship missile's terminal guidance law with multiple constraint based on back stepping. In Second International
10. Conference on Instrumentation, Measurement, Computer, Communication and Control, 892{895. IEEE. doi:10.1109/IMCCC.2012.214.